Sheffield Hallam University

A Homogenised Material Approach to Predict Fatigue Life of Additively Manufactured PLA with Different In-fill Levels

YAREN, Mehmet F. and SUSMEL, Luca

5th International Symposium on Fatigue Design and Material Defects FDMD 2025

A Homogenised Material Approach to Predict Fatigue Life of Additively Manufactured PLA with Different In-fill Levels

Mehmet F. Yaren[a], Luca Susmel[b,*]

[a]*Department of Mechanical Engineering, Sakarya University, 54050, Sakarya, Turkiye*

[b]*Materials and Engineering Research Institute (MERI), Sheffield Hallam University, Harmer Building, Sheffield, S1 1WB, United Kingdom*

Abstract

This study presents a novel fatigue life prediction method for plain and notched polylactide (PLA) structures manufactured with different in-fill levels via additive manufacturing. The proposed method models additively manufactured PLA with internal voids as a continuous, homogeneous, linear-elastic, and isotropic material. The effect of these voids is represented by an equivalent crack, whose size is related to the void size. This approach provides a practical and accurate way to estimate the fatigue life of both plain and notched components, even when manufactured with different in-fill levels. The predicted fatigue lives agree with the experimental results obtained from specimens in different raster angles and in-fill levels.

Keywords: Aadditive manufacturing; Polylactic acid (PLA); Voids; Fatigue; Critical distance; Notch

1. Introduction

Additive manufacturing (AM) makes it possible to create lightweight, complex, and custom parts that are difficult to create using conventional methods. However, as AM is a relatively new technology, further research is required to fully characterise the mechanical performance of printed components, particularly under cyclic loading.

Some studies have investigated the fatigue behaviour of PLA components produced by Fused Deposition Modeling (FDM), highlighting the effects of both design and manufacturing parameters. Hassanifard and Behdinan (2022) tested specimens printed flat on the build plate with unidirectional raster orientations (0° or 90°) and found that filament direction strongly affected fatigue life. The same study also showed that the raster angle affected the stress concentration around the notch. Ezeh and Susmel (2019) also printed specimens flat on the build plate but applied alternating raster patterns such as 0°/90° and -45°/45°. Their results indicated that variations in in-plane raster orientation had negligible effect on fatigue life. Cerda-Avila et al. (2023) printed parts in different build orientations. This change in geometric orientation, relative to the layer deposition direction, had a strong effect on fatigue life. It demon-

*
  Corresponding author. Materials and Engineering Research Institute, Sheffield Hallam University, Harmer Building, Sheffield, S1 1WB, UK *E-mail address:* l.susmel@shu.ac.uk (L. Susmel)
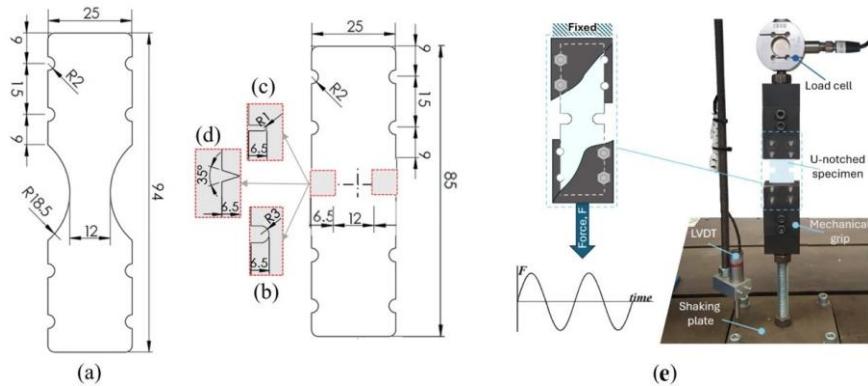
Fig. 1. Details of the specimens: (a) plain, (b) U-notched with 3 mm root radius, (c) U-notched with 1 mm root radius, (d) V-notched, and (e) experimental setup

strated that global build orientation is important. Regarding loading conditions, studies showed that non-zero mean stresses can significantly reduce fatigue life. PLA was found to be more sensitive to mean stress effects than traditional metals Algarni (2022); Ezeh and Susmel (2019). Manufacturing parameters such as nozzle diameter, printing speed, and extrusion temperature also affect fatigue performance. Lendvai et al. (2025) examined the effect of filament feed rate and showed that higher feed rates create larger internal voids. These voids increase stress concentrations and reduce fatigue strength. Rotating bending fatigue tests performed by Dadashi and Azadi (2023) revealed that decreasing the nozzle diameter and extrusion temperature enhances interlayer bonding, thereby improving fatigue performance. Similarly, Gomez-Gras et al. (2018) examined the effects of nozzle diameter, layer height, and fill density on fatigue performance, reporting that honeycomb in-fill outperforms rectilinear patterns under cyclic loading.

Most studies on FDM-printed PLA investigate the effect of manufacturing parameters through experiments, with limited focus on analytical methods. This paper builds on a previous study published in the International Journal of Fatigue by Yaren and Susmel (2025), which used the Theory of Critical Distances (TCD) Tanaka (1983);Taylor (1999) to assess the fatigue behaviour of PLA with different in-fill levels. That study introduced a method combining TCD with a homogenised cracked material concept to model internal voids. The method is reformulated to predict medium-cycle fatigue life using a simplified model: a homogenised continuous plate containing a central crack.

2. Additive manufacturing, experimental procedure, and results

The specimens were manufactured flat on the build plate using an Ultimaker® 2 Extended+ 3D printer with 2.85 mm white polylactic acid (PLA) filament from NewVerbatim®. The properties of the filament, as provided in its datasheet, include a density of 1.24 g/cm^3 and a glass transition temperature of 58°C. The yield strength of the parent material is specified as 63 MPa. Printing was performed using a 0.4 mm brass nozzle. The wall and shell thicknesses were set to 0.4 mm, with a layer height of 0.1 mm, a printing speed of 30 mm/s, a build plate temperature of 60°C, and an extrusion temperature of 210°C.

Plain and notched specimens, each with a thickness of 5 mm, were fabricated based on the technical drawings presented in Fig. 1a–d. It is worth mentioning that although the notch root radius for the V-notched specimen was

defined as zero in the technical drawings, optical measurements revealed that the actual root radius was approximately 0.15 mm.

Two types of internal geometries were investigated by varying the raster angles (θ_p) to 0°/90° and -45°/45°, each with five different in-fill levels (100%, 80%, 60%, 40%, 20%). Fig. 2 shows the internal geometries of the specimens corresponding to the different in-fill levels and illustrates the determination of the effective void size, d_v. Fig. 2 shows that d_v varies across the specimen, so an average from multiple measurements was used in subsequent calculations. For the notched specimens, d_v was generally measured around the notch, as crack initiation typically occurs in this area. Tabs. 1–2 present the measured values of d_v for each in-fill level and specimen type.
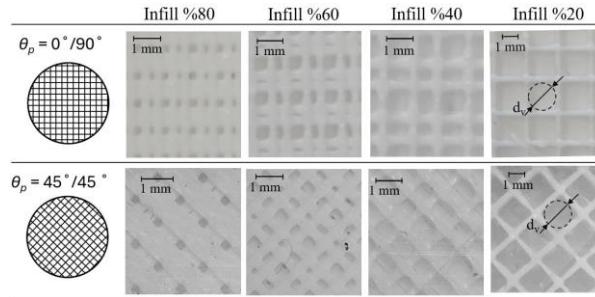

Fig. 2. Internal views of specimens by in-fill level (left to right) and raster angle (top to bottom); void size d_v is shown in the last column.

Table 1. The experimental results for un-notched specimens manufactured at different in-fill levels.

in-fill level [%]	R	θ_p [°]	$\Delta\sigma_{0-50\%}$ [MPa]	k	T_σ	N. of tests	d_v [mm]
100	-1	0	6.3	7.0	1.40	13	-
100	-1	45	5.5	8.0	1.50	7	-
100	0.1	0	3.9	8.4	1.42	12	-
80	-1	0	2.8	4.0	1.42	9	0.30
80	-1	45	3.8	6.1	1.49	9	0.26
80	0.1	0	2.5	7.7	1.21	9	0.30
60	-1	0	2.4	4.2	1.46	9	0.40
60	-1	45	2.7	5.3	1.47	8	0.53
60	0.1	0	1.7	6.2	1.34	9	0.40
40	-1	0	1.3	3.8	2.05	8	0.75
40	-1	45	2.6	8.3	1.37	8	0.84
40	0.1	0	0.9	4.1	1.53	11	0.75
20	-1	0	1.6	4.6	1.53	9	1.62
20	-1	45	1.8	6.1	1.65	10	1.60
20	0.1	0	0.8	4.5	1.58	9	1.62

Plain specimens were printed with two raster orientations, 0°/90° and -45°/45°, and tested under fully reversed loading ($R = -1$), while additional tests were performed on 0°/90° specimens under tensile–tensile loading ($R = 0.1$). Notched specimens were tested at both $R = -1$ and $R = 0.1$, but only with the 0°/90° raster angle. This decision was based on the observation that raster angle had no significant effect on the fatigue performance of plain specimens, allowing for a reduction in the number of tests with notched specimens.

The fatigue tests were conducted at room temperature under constant amplitude axial loading using a shaking table driven by an electric motor. Specimens were fixed to grips with bolts, as shown in Fig. 1e. An axial load cell and a linear variable differential transformer (LVDT) were used to measure and record force and displacement throughout the tests. Each test was terminated either upon specimen failure or upon reaching 2×10^6 cycles, which was considered as run-out.

A summary of the fatigue results for all test cases is presented in Tab. 1 for un-notched specimens and in Tab. 2 for notched specimens. Further details on the fatigue test data can be found in Ref. Yaren and Susmel (2025). In

calculating nominal stress for both notched and un-notched specimens, internal voids were not taken into account. Specifically, for the notched specimens, nominal stress was calculated based on the net cross-sectional area.

Tabs. 1 - 2 present the key fatigue parameters: $\Delta\sigma_{0-50\%}$, which is the stress range at the endurance limit for a 50% survival probability ($P_S = 50\%$), extrapolated at 2×10^6 cycles; the negative inverse slope (k) of the S–N curve; and the scatter ratio (T_σ). The scatter ratio is defined as the ratio of endurance limits at $P_S = 90\%$ and $P_S = 10\%$, assuming a log-normal distribution and estimated with a 95% confidence level. As summarised in Tabs. 1-2, increasing the in-fill level consistently led to a higher endurance limit across all combinations of load ratio, raster orientation, and geometry. Meanwhile, the negative inverse slope (k) remained approximately constant at around 5, regardless of the testing configuration.

Table 2. The experimental results for different type of notched specimens printed at different in-fill levels for $\theta_p = 0$.

Notch Type [%]	in-fill Level [%]	R	$\Delta\sigma_{0n,50\%}$ [MPa]	k_n	T_σ	N. of tests	d_v [mm]
V-notched	100	−1	2.5	3.9	1.17	8	
V-notched	100	0.1	2.2	5.6	1.64	8	-
V-notched	80	−1	2.7	5.6	1.55	8	
V-notched	80	0.1	2.0	6.5	1.22	8	0.20
V-notched	60	−1	1.8	4.8	1.31	8	
V-notched	60	0.1	1.6	5.4	1.71	9	0.39
V-notched	40	−1	1.4	4.4	1.76	8	
V-notched	40	0.1	1.1	5.1	1.44	9	0.73
V-notched	20	−1	1.5	5.4	1.59	8	
V-notched	20	0.1	1.5	7.6	1.33	6	1.57
U-notch, 1 mm root radius	100	−1	3.3	4.7	1.43	7	-
U-notch, 1 mm root radius	100	0.1	2.6	6.8	1.27	8	-
U-notch, 1 mm root radius	80	−1	2.6	5.0	1.20	8	0.23
U-notch, 1 mm root radius	80	0.1	1.9	5.7	1.39	8	
U-notch, 1 mm root radius	60	−1	1.5	3.7	1.80	10	0.38
U-notch, 1 mm root radius	60	0.1	1.5	5.5	1.60	8	
U-notch, 1 mm root radius	40	−1	1.3	4.5	1.47	7	0.75
U-notch, 1 mm root radius	40	0.1	1.2	6.4	1.27	8	
U-notch, 1 mm root radius	20	−1	1.2	5.7	1.28	7	1.66
U-notch, 1 mm root radius	20	0.1	1.0	6.4	1.14	8	
U-notch, 3 mm root radius	100	−1	4.6	5.8	1.29	10	-
U-notch, 3 mm root radius	100	0.1	2.8	5.4	1.53	8	-
U-notch, 3 mm root radius	80	−1	2.6	4.0	1.36	8	0.23
U-notch, 3 mm root radius	80	0.1	2.4	6.1	1.69	8	
U-notch, 3 mm root radius	60	−1	2.7	7.9	1.24	8	0.42
U-notch, 3 mm root radius	60	0.1	1.4	4.1	1.50	9	
U-notch, 3 mm root radius	40	−1	1.9	6.5	1.41	9	0.77
U-notch, 3 mm root radius	40	0.1	1.4	6.2	1.31	8	
U-notch, 3 mm root radius	20	−1	1.6	5.8	1.19	8	1.66
U-notch, 3 mm root radius	20	0.1	1.0	5.2	1.63	8	

3. Fatigue life estimation of additively manufactured plain and notched specimens

The approach proposed in this section to estimate the fatigue life of AM PLA structures is based on some assumptions based on experimental findings on previous studies Ezeh and Susmel (2019), Ahmed and Susmel (2019).

First, since the effect of raster angle on fatigue life is considered negligible for specimens printed flat on the build plate, the material behaviour can be assumed homogeneous and isotropic. Additionally, the stress–strain behaviour of the PLA specimens is assumed to be linear-elastic, and the effect of superimposed static stresses on fatigue performance is accounted for by the maximum stress in each loading cycle.

3.1. Life estimation on un-notched specimen

As shown in Tab. 1, a decrease in in-fill density reduces the fatigue strength of 3D-printed PLA, making void size an important factor in fatigue life estimation. Fig 3a illustrates a PLA un-notched structure that contains internal voids of size d_v, subjected to cyclic tensile loading. The structure fails after N_f cycles. It should be noted here that the internal voids are neglected in stress calculations, meaning that the structure is made from homogeneous and continuous material.

Fig. 3b illustrates an infinitely large plate, made of a continuous, homogeneous, isotropic, and linear-elastic material, containing a centrally located through-thickness crack with a half-length a_{eq}, and subjected to cyclic loading. In this context, the equivalent crack length a_{eq} corresponds to the crack size that leads to failure of the plate after N_f cycles under the applied maximum stress σ_{max}. Since the configuration shown in Fig. 3b is considered as a central through-thickness crack, the Linear Elastic Fracture Mechanics (LEFM) shape factor is independent of crack length
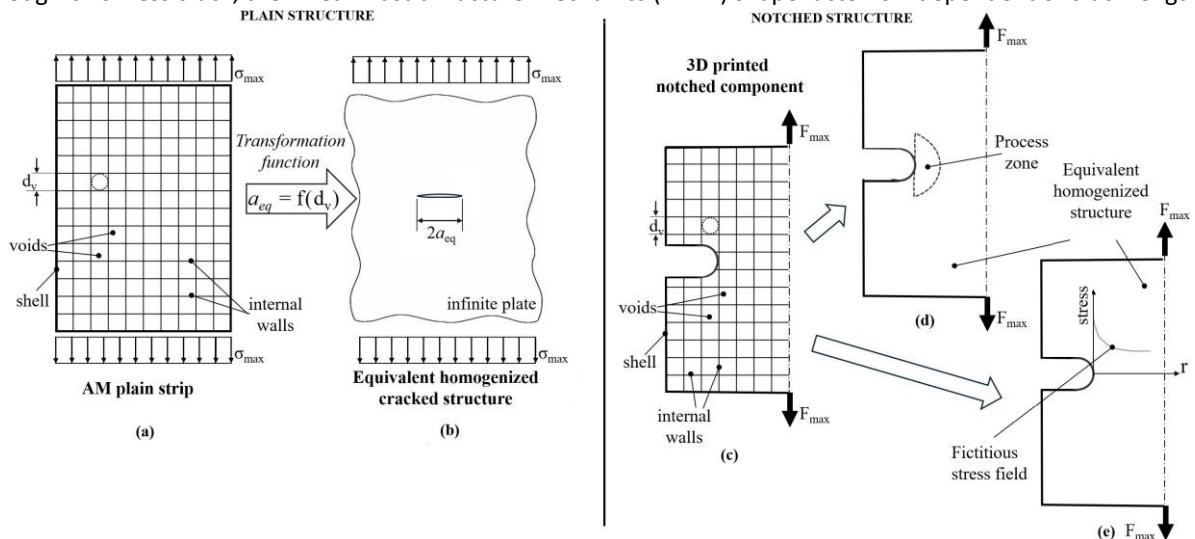
Fig. 3. Illustration of the transformation from a plain material with uniformly distributed voids (a) to an equivalent homogenized cracked continuum material (b); process zone (c) and fictitious linear-elastic local stress fields (e) to estimate fatigue lifetime of notched components (d) of AM PLA

and equals 1. Additionally, the structures shown in Figs. 3a and b are assumed to exhibit the same fatigue strength in the case of 100% in-fill and absence of any cracks. To achieve identical fatigue lives (N_f) under cyclic loading with a maximum stress of σ_{max} for both the plate containing a central through-thickness crack and the un-notched plate with internal voids, a relationship between the equivalent half-crack length (a_{eq}) and the internal void size (d_v) must be established. In Eq. (1), the function f(d_v) transforms the AM plate with internal voids (Fig. 3a) into an equivalent homogeneous, isotropic, linear-elastic plate containing a central crack, as depicted in Fig. 3b.

$$a_{eq} = f(d_v) \tag{1}$$

The Theory of Critical Distances (TCD), as given in Eqs. (2) and (3), is used to evaluate the fatigue strength of an infinite plate with a through-thickness crack under cyclic tensile loading.

$$\Delta\sigma_{0n} = \Delta\sigma_o \left[1 - \left(\frac{a}{a + \frac{L}{2}}\right)\right]^2 \tag{2}$$

$$\Delta\sigma_{0n} = \Delta\sigma_o \sqrt{\frac{L}{a + L}} \tag{3}$$

By replacing the a in Eqs. (2) and (3) with the a_{eq} and using the critical distance $L_M(N_f)$, the PM and LM can be directly expressed as follows for PM (Eq. 4) and LM (Eq. 5). For a detailed definition of critical distance for fatigue loading $L_M(N_f)$, readers are referred to the paper by Susmel and Taylor (2007).

$$\sigma_{max} = \sigma_{max,0} \cdot \left(\frac{N_{Ref}}{N_f}\right)^{!k}_{100\%} \cdot \left[1 - \left(\frac{a_{eq}}{a_{eq} + \frac{|L_M(N_f)|_{100\%}}{2}}\right)\right]^2 \tag{4}$$

$$\sigma_{max} = \sigma_{max,0} \cdot \left(\frac{N_{Ref}}{N_f}\right)^{!k}_{100\%} \cdot \sqrt{\frac{L_M(N_f)_{100\%}}{a_{eq} + L_M(N_f)_{100\%}}} \tag{5}$$

In Eqs. (4) and (5), $\sigma_{max,0}$ represents the endurance limit at N_{Ref} cycles, and k is the negative inverse slope of the fatigue curve obtained from specimens manufactured with 100% in-fill. Notably, these equations are expressed in terms of the maximum stress in the fatigue cycle, as experimental study Ezeh and Susmel (2019) has shown that the maximum stress effectively captures the influence of mean stress on the fatigue performance of additively manufactured PLA.

As previously mentioned in Eq. (1), to define the relationship between the equivalent half-crack length a_{eq} and the void size d_v in the simplest form, a linear function can be assumed. Accordingly, the relationship can be expressed using a dimensionless transformation constant k_t as follows:

$$a_{eq} = k_t \cdot d_v \tag{6}$$

After directly determining the constant k_t from experiments on specimens with less than 100% in-fill, it can be substituted into Eqs. (4) and (5). Now the Point Method (PM) and Line Method (LM) methods in TCD can be applied by using the Eqs. (7) and (8).

$$\sigma_{max} = \sigma_{max,0} \cdot \left(\frac{N_{Ref}}{N_f}\right)^{!k}_{100\%} \cdot \left[1 - \left(\frac{k_t \cdot d_v}{k_t \cdot d_v + \frac{A \cdot N_{f\,100\%}^{B}}{2}}\right)\right]^2 \tag{7}$$

$$\sigma_{max} = \sigma_{max,0} \cdot \left(\frac{N_{Ref}}{N_f}\right)^{!k}_{100\%} \cdot \sqrt{\frac{A \cdot N_{f\,100\%}^{B}}{k_t \cdot d_v + A \cdot N_{Bf}}} \tag{8}$$

In Eqs. (7) and (8), σ_{max} is the maximum stress in the fatigue cycle applied to the un-notched AM component being designed (Fig. 3a). The stress analysis is conducted assuming the material is linear-elastic, continuous, homogeneous, and isotropic (i.e., by neglecting the presence of manufacturing voids). Fatigue constants $\sigma_{max,0}$ (at N_{Ref} cycles to failure), k, A, and B are all determined by testing specimens manufactured by setting the in-fill level equal to 100%.

In Eqs. (7) and (8), A and B are material constants that must be determined experimentally. Although the values of A and B for a specific material may vary with changes in the load ratio, they remain unaffected by variations in the profile or the sharpness of the geometrical feature being assessed Susmel and Taylor (2007). For a detailed definition of critical distance for fatigue loading $L_M(N_f)$, the constants A and B, readers are referred to the paper by Susmel and Taylor (2007). As a result, the PM and LM approaches can be used to estimate fatigue life by solving Eqs. (7) and (8) for N_f. The corresponding number of failure cycles can be efficiently computed using conventional numerical methods.

3.2. Life estimation on notched specimen

Localized stress concentrations within AM structures can compromise structural integrity. To overcome this issue, a combined approach integrating the TCD and the previously introduced equivalent homogeneous material modeling is proposed. This framework enables the fatigue strength of notched AM PLA components to be assessed through simple and reliable design rules. As shown in Fig. 3c, a notched AM component with less than 100% in-fill contains internal voids with an average size of d_v and is subjected to uniaxial fatigue loading with a peak cyclic force F_{max}.

To accurately estimate the fatigue strength using the TCD, the notched AM component shown in Fig. 3e is modeled as a continuous, homogeneous, isotropic, and linear-elastic body with the same dimensions as the component in Fig. 3d. This approach enables the application of the Point Method (PM) and the Line Method (LM), assuming that the size of the process zone remains constant regardless of internal void size in Fig. 3c. Based on this assumption, the critical distance L_M from fatigue tests on plain specimens with 100% in-fill is calculated by using the proposed approach by Susmel and Taylor (2007). Since L_M is constant for a given AM material, the influence of manufacturing voids is considered by adjusting the intrinsic static strength of the material using either Eqs. (7) and (8).

Assuming the AM component behaves as a continuous, homogeneous, isotropic, and linear-elastic material, the local fictitious stress fields shown in Fig. 3e can be determined using standard Finite Element (FE) analysis or analytical methods. These stress fields are used to calculate the effective stress $\sigma_{max,eff}$ using either the PM or LM from TCD. To account for internal voids, the fatigue failure condition at N_f cycles is given by:

$$\sigma_{eff,max} N_f = \sigma_{max} N_f \tag{9}$$

Here, $\sigma_{max,eff}(N_f)$ is the fatigue strength of the plain material, evaluated using Eqs. (7) and (8), both expressed in terms of maximum stress to include mean stress effects. For the PM, the failure condition can be directly obtained by combining the effective stress definition in Eq. (10) with the fatigue strength model in Eq. (7). Similarly, for the LM, it is derived by combining Eq. (10) with Eq. (8).

$$\Delta\sigma_{eff} = \Delta\sigma_y\left(\theta = 0, r = \frac{L_M(N_f)}{2}\right) \tag{10}$$

$$\Delta\sigma_{eff} = \frac{1}{2 \cdot L_M(N_f)} \int_0^{2L_M(N_f)} \Delta\sigma_y(\theta = 0, r) \cdot dr \tag{11}$$

$$\sigma_{y,max}(\theta = 0, r) = \frac{A \cdot N^{B}_{f\,100\%}}{2 \cdot A \cdot N^{Bf}_{100\%}} \cdot f_{100\%} = \sigma_{max,0} \cdot \frac{N_{Reff}}{k_t \cdot d_V + A \cdot N^{Bf}_{100\%}} \cdot k_{100\%} \cdot tu$$

$$1 \quad Z_{2 \cdot A \cdot Nbf\,100\%} \quad 1 - \left[\frac{k_t \cdot d_V}{k_t \cdot d_V + \frac{A \cdot N^{B}_{f\,100\%}}{2}} \right]^2 \tag{12}$$

$$\sigma_{y,max}(\theta = 0, r) \cdot dr = \sigma_{max,0} \cdot \frac{N_{Ref}}{} \cdot {}^k \cdot \frac{A \cdot N^{B}_{f\,100\%}}{} \tag{13}$$

Eqs. (12) and (13), the unknown is the number of cycles to failure, N_f, which appears on both sides of the equations. To find the fatigue life, standard numerical iteration methods can be used by combining the linear-elastic fictitious stress field with the PM and LM formulations in Eqs. (12) and (13), respectively.

4. Model validation with experimental results

Local stress fields for the TCD analysis were obtained using 2D linear-elastic FE models (PLANE182) in ANSYS®. The notched AM-PLA specimens were modeled as homogeneous, isotropic, and linear-elastic materials, without explicitly including internal voids. In the simulations, the root radius of V-notch was set to 0.15 mm, matching the average measured value from the actual manufactured specimens. To assess the accuracy and reliability of the Point Method (PM) and Line Method (LM), Eqs. (7) and (8) were employed to estimate the fatigue strength of the un-notched specimens (see Tab. 1).

The required constants A and B in these equations, which are used to define the critical distance for fatigue loading $L_M(N_f)$, were derived from fatigue test results of 100% in-fill plain and V-notched specimens Fig. 1a and d. Key parameters of the fatigue curves are presented in Tabs. 1 and 2. The resulting values for A and B were 25.1 and -0.242, respectively.

Then, experimental results from plain PLA specimens printed with 80% in-fill and a raster angle of $(\theta_p) = 0°$ under fully reversed loading (R = -1) were used to calibrate the transformation function $f(d_V)$ in Eq. (6). For each data point, the number of cycles to failure (N_f) was taken from the experiment, and the transformation constant k_t was calculated using both the PM and LM approaches defined in Eqs. (7) and (8). The average of the eight calculated k_t values gave 9.4 for the PM and 8.2 for the LM.

Due to page limits, Fig. 4a and b show PM and LM results for one un-notched and one notched case, respectively, though both methods were validated for all specimen types. In Fig. 4a, the PM predictions using Eqs.(7) and (8) show strong agreement with experimental fatigue lives for un-notched specimens, with most data points falling within the scatter band of the 100% in-fill reference curve. Similarly, Fig. 4b illustrates that the LM predictions from Eqs.(12) and (13) also align closely with the experimental results for notched specimens. These results confirm the accuracy and consistency of the proposed TCD-based framework in predicting fatigue life for both notched and un-notched AM PLA components with various in-fill levels. Since the method relies on linear-elastic FE stress fields using a homogeneous, isotropic material model, it avoids the need to explicitly model internal voids, making it practical for fatigue design of AM components.
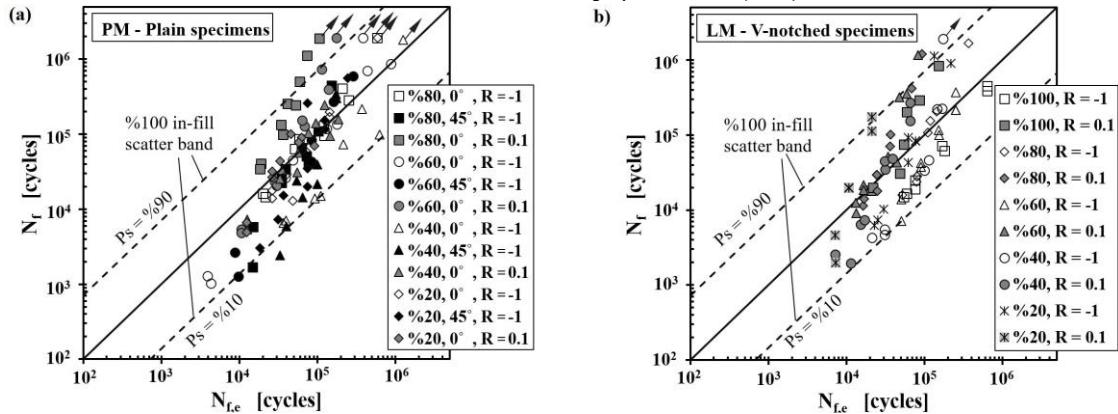
Fig. 4. Accuracy of (a) PM for plain and (b) LM for V-notched specimens in estimating the fatigue life of AM PLA with different infill levels.

5. Conclusion

This study experimentally and computationally investigates the effect of in-fill level on the fatigue performance of plain and notched AM PLA. A new approach based on the TCD is proposed to estimate the fatigue behaviour of both additively manufactured plain and notched PLA, accounting for internal voids. A strong correlation between internal void size and the fatigue strength of plain AM PLA is established by using an equivalent homogenised material concept within the TCD framework. The proposed approach also yields accurate fatigue life predictions for notched components manufactured with varying in-fill levels. The proposed TCD-based fatigue design method allows the use of standard linear-elastic FE results from homogeneous, isotropic models, removing the need to model manufacturing voids explicitly.

References

Ahmed, A.A., Susmel, L., 2019. Static assessment of plain/notched polylactide (pla) 3d-printed with different infill levels: Equivalent homogenised material concept and theory of critical distances. Fatigue & fracture of engineering materials & structures 42, 883–904.

Algarni, M., 2022. Fatigue behavior of pla material and the effects of mean stress and notch: Experiments and modeling. Procedia Structural Integrity 37, 676–683.

Cerda-Avila, S.N., Medellín-Castillo, H.I., Cervantes-Uc, J.M., May-Pat, A., Rivas-Menchi, A., 2023. Fatigue experimental analysis and modelling of fused filament fabricated pla specimens with variable process parameters. Rapid Prototyping Journal 29, 1155–1165.

Dadashi, A., Azadi, M., 2023. Experimental bending fatigue data of additive-manufactured pla biomaterial fabricated by different 3d printing parameters. Progress in Additive Manufacturing 8, 255–263.

Ezeh, O., Susmel, L., 2019. Fatigue strength of additively manufactured polylactide (pla): effect of raster angle and non-zero mean stresses. International Journal of Fatigue 126, 319–326.

Gomez-Gras, G., Jerez-Mesa, R., Travieso-Rodriguez, J.A., Lluma-Fuentes, J., 2018. Fatigue performance of fused filament fabrication pla specimens. Materials & Design 140, 278–285.

Hassanifard, S., Behdinan, K., 2022. Effects of voids and raster orientations on fatigue life of notched additively manufactured pla components. The International Journal of Advanced Manufacturing Technology 120, 6241–6250.

Lendvai, L., Fekete, I., Rigotti, D., Pegoretti, A., 2025. Experimental study on the effect of filament-extrusion rate on the structural, mechanical and thermal properties of material extrusion 3d-printed polylactic acid (pla) products. Progress in Additive Manufacturing 10, 619–629.

Susmel, L., Taylor, D., 2007. A novel formulation of the theory of critical distances to estimate lifetime of notched components in the medium-cycle fatigue regime. Fatigue & Fracture of Engineering Materials & Structures 30, 567–581.

Tanaka, K., 1983. Engineering formulae for fatigue strength reduction due to crack-like notches. International Journal of Fracture 22, R39–R46.

Taylor, D., 1999. Geometrical effects in fatigue: a unifying theoretical model. International journal of fatigue 21, 413–420.

Yaren, M.F., Susmel, L., 2025. A novel critical distance-based homogenised material approach to estimate fatigue lifetime of plain/notched polylactide 3d-printed with different in-fill levels. International Journal of Fatigue 193, 108750.